Int. J. Nonlinear Anal. Appl. 16 (2025) 4, 295–309
ISSN: 2008-6822 (electronic)
http://dx.doi.org/10.22075/ijnaa.2023.30984.4532

A newly proposed super-twisting backstepping sliding mode controller

Mostafa Rabbani, Reihaneh Kardehi Moghaddam*

Department of Electrical Engineering, Mashhad branch, Islamic Azad University, Mashhad, Iran

(Communicated by Mouquan Shen)

Abstract

The chattering phenomenon has been one of the most important controlling challenges in recent years, and efforts have been made to eliminate or control this phenomenon effectively, with various control strategies. In this article, a new super-twisting back-stepping sliding mode controller is proposed and to validate the performance of this controller, the outcomes of some well-known techniques are compared, in two aspects reducing tracking error and removing the chattering phenomenon. Also, a comparative analysis between control methods such as sliding mode, feedback linearization and back-stepping control has been done in the sense of stability and convergence. The model discussed in this article is a non-linear, highly unstable system of the inverted pendulum. The results of applying the proposed controller on an inverted pendulum are compared in terms of the tracking speed, convergence time, error and chattering reduction. In addition, the stability analysis of the closed-loop system is presented according to the Lyapunov theorem. The results clearly show the efficiency of the proposed method not only in terms of stability and convergence improvement but also in reducing unwanted chattering.

Keywords: Sliding mode, Chattering, Feedback linearization, Back Stepping, Control, Inverted pendulum
2020 MSC: 34Hxx

1 Introduction

In recent years, many researchers have studied various control methods on highly nonlinear and unstable systems, including the inverted pendulum. Design of an efficient controller with suitable performance requires good calculations, the designer's precise understanding of the controller, and examination of the issues. In this paper a newly proposed super twisting back-stepping sliding mode control (SMC) is defined and the performance has been shown for problems such as non-linear interference interpretation, error reduction and control adjustment.

In recent years different strategies have been proposed to extend and improve the efficiency of sliding mode controllers in [17], an improved sliding model method is introduced that shows good performance in error removal and tracking speed. In [35, 39], the development strategy with adaptive sliding mode control is implemented on the inverted pendulum system and Unmanned Surface Vehicle. In [17], a kind of non-contact vibration measurement method for a two-connected flexible piezoelectric plate using laser sensors is proposed and used method of fuzzy sliding mode to solve this problem. In [28], with the help of adjusting the sliding mode controller, a robust mode has been created. In [10], a sliding mode control system is designed for control under pressure nuclear water reactor (PWR) power. In

*Corresponding author
Email addresses: m.rabbani@mshdiau.ac.ir (Mostafa Rabbani), r_k_moghaddam@mshdiau.ac.ir (Reihaneh Kardehi Moghaddam)

Received: June 2023 *Accepted:* November 2023

[41], the sliding mode control method is used to extract the maximum power from wind energy. Many studies have been done to design the controller with the linearization method around the fixed point of the system [11].

In these studies, the feedback linearization method has been compared with the standard sliding mode control method. In [48], the controller examines the sliding model along with a new sliding surface in the presence of disturbance. In [20] the method of super twisting sliding mode has been used to solve the problem of the maximum power point of PT in the application of new MP energies such as solar energy. In [43], the standard sliding mode controller is used to control the mode changes of the inverted pendulum.SMC sliding mode controllers and their improved versions propose good dynamic response and disturbance robustness, consequently they are implemented on many real-world industrial systems [31].

In [23], an adaptive sliding mode control to control chaotic systems is proposed. In [44], to solve the path tracking problem with unknown uncertainties, a new controller consisting of the a proportional-integral-differential sliding mode surface (PIDSM) and the rate of progress of the hyperbolic reaching law is proposed. In [29], the control of the permanent magnet synchronous motor, which is a non-linear industrial system, is performed by sliding mode. In [15], the developed sliding mode controller is used to improve the performance of the wind energy conversion system caused by the permanent magnet synchronous generator and increase the quality of electricity to the network and subscribers. In [22], the survey and review of the sliding mode controller for network control systems has been analyzed and reviewed. In [26] terminal sliding mode control is used to adjust the servo speed of permanent magnet motor. Also, in new researches, a control strategy on the terminal sliding mode controller has been proposed for industrial nonlinear systems [49] and linear [42].

In [4], the performance of the sliding mode control method for the synchronization of fractional order chaotic systems has been investigated. In [21], the terminal sliding mode control method has been implemented and implemented on a real four-rotor unmanned ticket system. In [19, 34], with the help of the method of pole placement and state linearization, feedback linearization and input linearization, the nonlinear system of the inverted pendulum is stabilized. In [24], the sliding mode control was developed for the DC-DC buck converter system and in [45] this method is used to control the robot with two arms.

The sliding mode controller method can also be used for viscous fluid control systems that have a non-linear method [36]. In [49, 5], he used the Super Twisting sliding mode method and its developed versions, including adaptive and fuzzy, to remove the chattering phenomenon and control the inverse pendulum. The combined Back-stepping Super-Twisting algorithm for speed control of a three-phase induction motor is studied in [6]. Back stepping control method for many industrial applications, including power point tracking in photovoltaic systems [13], helicopter control [12], UPS uninterruptible power source control [38], reverse pendulum control [16] and [7] and tracking Quadrature route [14, 3]. In recent researches, developed sliding mode controlling methods such as Adaptive fuzzy fast terminal sliding mode control [46] and PID-Sliding mode controller [45] have been proposed and utilized to stabilize the inverted pendulum. Also, hybrid structures, including the Adaptive backstepping integral sliding mode control [2] for independent excitation dc motor speed control, a sliding mode based on super-twisting sliding mode control [25] for guiding unmanned surface vehicles and backstepping based sliding mode control for load frequency control in power systems [9] is of interest to many researchers.

The superiority of the method proposed in this article is proposing a newly proposed backstepping-sliding mode structure that considers all implementation limitations including tracking error, chattering phenomenon in the control signal, speed of convergence simultaneously and leads to a good performance in compare with similar controlling structures. The main body of this article consists of four parts. In the first part, the systems dynamic is expressed. In the second part, of the controller is designed based on feedback linearization method. The third part of the article deals with design of sliding mode controller, its related stability proof and controller improvement which yields chattering reduction. Forth part proposes the back stepping super twisting sliding mode method. The final section contains comparative analysis of proposed method, feedback linearization and sliding mode controlling.

2 Methodology

Consider a special class of second order nonlinear systems with canonical structure as follow:

$$\begin{cases} \dot{x}_1 = x_1 \\ \dot{x}_2 = f(x,t) + g(x,t)u + d(t) \end{cases} \tag{2.1}$$

Where f and g are non-linear Lipschitz functions which can include bounded parametric uncertainties. u is the input control signal,$x = [x_1, x_2]^T \in \mathbb{R}^n$ is the system states and $d(t)$ is the disturbance function which satisfies $d(t) \leq \|D\|$

Definition 2.1. The function $f : \mathbb{R}^n \to \mathbb{R}^m$ is locally Lipshitz at $x_0 \in \mathbb{R}^n$, if there exists:

- A neighborhood $B(x_0, \varepsilon) = \{x \in \mathbb{R}^n | \, \|x - x_0\| < \varepsilon\}$ with $\varepsilon > 0$
- Lipschitz constant $L > 0$

So that the following condition is satisfied.

$$\forall x \in B(x_0, \varepsilon), \|f(x_1) - f(x_2)\| \leq L \|x_1 - x_2\|$$

To clarify the method without losing the generality in the next section the inverted pendulum system which is an example of proposed class is considered.

2.1 Inverted Pendulum System Equations

Figure 1 shows and inverted pendulum structure. Mathematical equations and dynamic model representing the

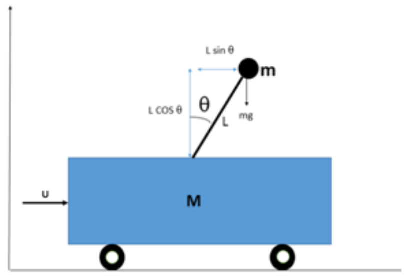

Figure 1: Physical model of inverted pendulum

behavior of the inverted pendulum system are explained by equations 2.1 and 2.2. As can be seen, this system has strongly nonlinear terms. The values of the parameters of the inverted pendulum system in performing calculations and simulations are as described in Table No. 1.

Table 1: System parameters of inverted pendulum.

Parameter	value Parameter	Symbol
M	Cart mass	1kg
m	Pendulum mass	0.1kg
g	Acceleration of gravity	9.8 m/s2
L	Half length of the pendulum	0.5m

$$\begin{cases} \dot{x}_1 = x_2 \\ \dot{x}_2 = f(x_1, x_2) + b(x_1, x_2) u \end{cases}, \dot{x} = \begin{bmatrix} \theta \\ \dot{\theta} \end{bmatrix}$$

$$\begin{cases} f(x_1, x_2) = \dfrac{(M + m) g \sin x_1 - mLx_2^2 (\sin x_1 \cos x_1)}{\frac{4}{3}(M + m) L - mL\cos^2 x_1} \\ b(x_1, x_2) = \dfrac{\cos x_1}{\frac{4}{3}(M + m) L - mL\cos^2 x_1} \end{cases} \tag{2.2}$$

where functions f and b are non-linear equations expressed in the form of equation 2.2. As can be seen from Figure 2, despite the difference in the initial conditions of the system states, the states converge to an oscillatory cycle.

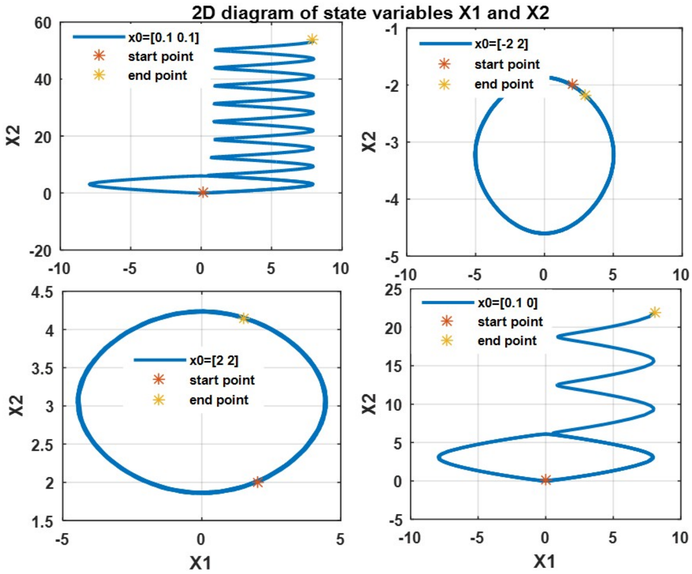

Figure 2: Dynamic limit cycle of the nonlinear inverted pendulum system for different initial conditions

2.2 Controller design based on feedback linearization

In this section, the feedback linearization strategy is used to linearize the nonlinear equations of the inverted pendulum. Considering the canonical form, it is possible to linearize the non-linear system by using a quasi-linear controller and guarantee the control and stability of both system output variables and reference signal tracking in the tracking operation. According to the canonical structure of system state equations, the controller signal is proposed as equation 2.3.

$$u = \frac{1}{b}\left(-f+v\right) \Rightarrow u = \frac{\frac{4}{3}\left(M+m\right)L - mL\cos^2 x_1}{\cos x_1}\left(-\frac{\left(M+m\right)g\sin x_1 - mLx_2^2\left(\sin x_1 \cos x_1\right)}{\frac{4}{3}\left(M+m\right)L - mL\cos^2 x_1} + v\right) \tag{2.3}$$
$$\rightarrow \dot{x}_2 = v$$

The virtual controller v for the virtual linearized system is in the form of equation 2.4.

$$v = x_d^n - k_{n-1} \quad e^{n-1} \quad .....k_1\dot{e} - k_0 e \Rightarrow e^n + \ k_{n-1} \quad e^{n-1} + ...k_1\dot{e} - k_0 e = 0 \tag{2.4}$$

In equation 2.4, n is the number of system states, which is equal to 2, and e is the error signal and x_d is the input reference signal.

$$v = \ddot{x}_d - k_1\dot{e} - k_0 e \Rightarrow \ddot{e} + k_1\dot{e} + k_0 e = 0 \tag{2.5}$$

$$s^2 + k_1 s + k_0 = 0 \tag{2.6}$$

We rewrite equation 2.5 as 2.6. The coefficients K_1 and K_2 determine the location of the closed loop poles of the system. Finally, the virtual controller is determined as equation 2.7.

$$v = -k_1 x_1 - k_2 x_2 \tag{2.7}$$

States dynamics and controlling signal extracted from feedback linearization method are illustrated in figures 3.a and 3.b respectively. To guarantee the stability K_1 and K_2 It should be determined in such a way as to guarantee the Hurwitz property of polynomial 6. Accordingly we suppose $K_1 = K_2 = 10$, $X_0 = [0.2, 0.1]$ and $X_d = \frac{\pi}{30}\sin(t)$.

Also the tracking error related to state X_1 and X_2 is shown in Figure 4 and Figure 5. As it is mentioned the error converges to zero in about 5 seconds.

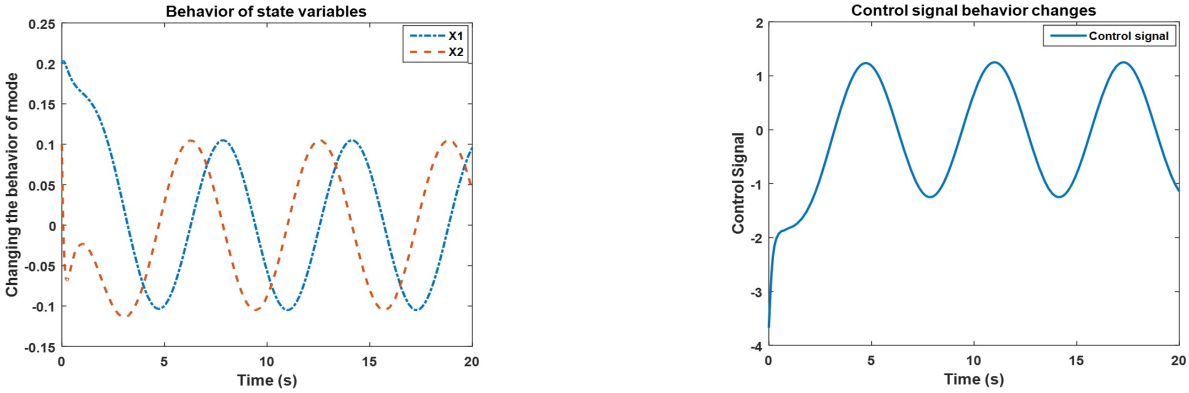

Figure 3: state variables x_1 and x_2 and controlling signal

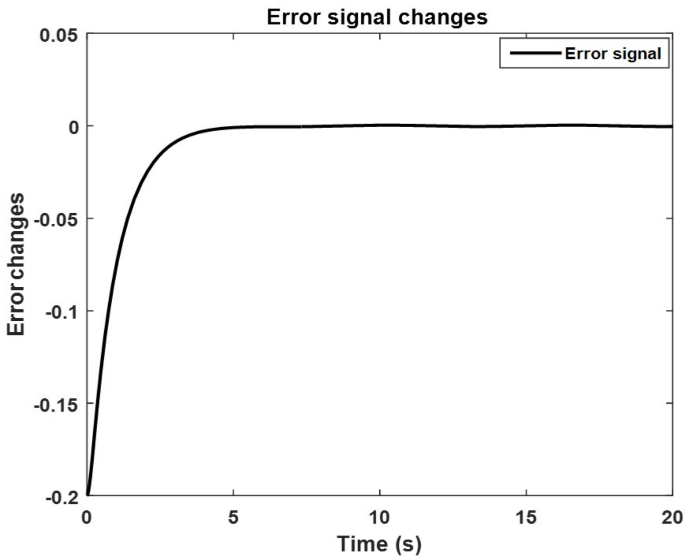

Figure 4: error signal obtained by feedback linearization method

2.3 Controller design based on sliding mode control

Consider the nonlinear structure of 2.2 and also the standard sliding surface which is a function of tracking error is defined as follows where λ is a positive constant.

$$s = \left(\frac{d}{dt} + \lambda\right)^1 e = \dot{e} + \lambda e \tag{2.8}$$

To guarantee the lyapunov stability and also finite time convergence to sliding surface, the following equation must be satisfied.

$$s\dot{s} \le -\mu \left| s \right| \tag{2.9}$$

The SMC controller is defined as follows, where $\hat{U}$ is the nominal part and U_{SW} is the variable structure obtained from reachability condition 2.9.

$$u = \hat{U} - U_{SW}; \quad U_{SW} = ksign\left(s\right)$$

$$\hat{U} = \frac{-1}{\mathrm{b}}(q + \ ksign\left(s\right)) = \frac{-\frac{4}{3}\left(M + m\right)L - mL\cos^2 x_1}{\cos x_1}(q + \ ksign\left(s\right)); \quad q = \lambda\left(x_{2-}\ \dot{x}_d\right) + \left(f - \ddot{x}_d\right)$$

$$\to q = \lambda\left(x_{2-}\ \dot{x}_d\right) + \left(\frac{\left(M + m\right)g\sin x_1 - mLx_2^2\left(\sin x_1 \cos x_1\right)}{\frac{4}{3}\left(M + m\right)L - mL\cos^2 x_1} - \ddot{x}_d\right). \tag{2.10}$$

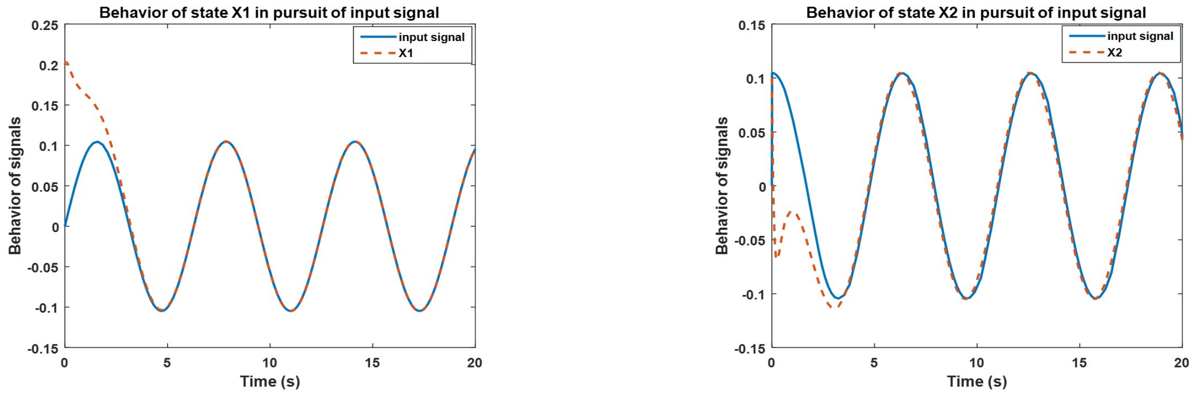

Figure 5: X_1 and X_2 reference tracking error obtained by feedback linearization method

Table 2: Literature review to reduce chattering

Reference	Variable structure part	Details
[1, 11, 31, 45, 36, 5, 46, 33]	$U_{SW}=-Ksign(s)$	$sign(s)=\frac{s}{\lvert s\rvert}$ $sign(s)=0$
[15]	$U_{SW}=-Kep.sign(s)$	$sign(s)=\frac{s}{\lvert s\rvert+\epsilon}$
[40, 33]	$U_{SW}=-K.sat(s)$	$sat(s)=\left\{\begin{array}{cc} -1 & s<-\phi \\ \frac{s}{\phi} & -\phi\leq s\leq\phi \\ 1 & s>0 \end{array}\right\}$ $0<\phi<1$
[44]	$U_{SW}=-K\tanh(s)$	...
[10, 45]	$U_{SW}=-K.\tanh(\frac{s}{\delta})$	$\delta=0.5$
[20, 30, 33]	$U_{ST}=-\alpha\lvert s\rvert^{2}sign(s)+U_1,\dot{U}_1=-\omega sign(s)$	$\alpha=2,p=0.5,\omega=8$
[39]	$U_{SW}=-K\tanh(\rho s),K>0$	$\tanh(\rho s)=\frac{e^{\rho s}-e^{-\rho s}}{e^{\rho s}+e^{-\rho s}}$ $\rho>0$

Considering $k=18$ and $\lambda=5$; the inequality 2.9 and consequently stability will be satisfied:

$$s\left(\lambda\left(\dot{x}_1-\dot{x}_{d_1}\right)+\left(\dot{x}_2-\ddot{x}_{d_1}\right)\right)\leq-\mu\left|s\right|$$

$$\begin{array}{l} s\left(\lambda\left(\dot{x}_1-\dot{x}_{d_1}\right)+\left(\dot{x}_2-\ddot{x}_{d_1}\right)\right)\leq-\mu\left|s\right| \\ s\left(\lambda\left(x_2-\dot{x}_{d_1}\right)+\left(f+bu-\ddot{x}_{d_1}\right)\right)\leq-\mu\left|s\right| \\ s\left(\lambda\left(x_2-\dot{x}_{d_1}\right)+\left(\frac{(M+m)g\sin x_1-mLx_2^2(\sin x_1\cos x_1)}{\frac{4}{3}(M+m)L-mL\cos^2 x_1}+\frac{\cos x_1}{\frac{4}{3}(M+m)L-mL\cos^2 x_1}u-\ddot{x}_{d_1}\right)\right)\leq-\mu\left|s\right|. \end{array}$$

One of the classic SMC problems in industrial implementation is the presence of unwanted and annoying chattering fluctuations which causeincreasing control activity, inducing unmolded high-frequency dynamics, reducing control accuracy, increasing heat losses in electrical circuits, and electrical energy consumption in mechanical parts and actuators. Accordingly, the controller 2.10 is improved through Table 2.

In the sequel the sliding surface and controlling signals for inverted pendulum are discussed using methods mentioned in above table.

As seen in the above table, using the sign function causes drastic changes in the control signal, which causes damage to industrial equipment, and improved controlling signals greatly reduce chattering. In Table 4, the different methods presented in Table 3 are compared in terms of the time to converge to the sliding surface with an error of less than $e=0.0001$.

According to Table 4, the state variables in the supertwisting method reach the sliding surface in less than 2s and are attracted to this surface. In the following, it is shown that the absorption of the state variables to the sliding surface is effective in the operation of following the reference signal, and there is less error between the values of the

Table 3: Sliding surface and controlling signals after applying Table 2 controlling strategies on inverted pendulum

Variable structure	Control Signal	Sliding surface
$U_{SW} = -Ksign(s)$	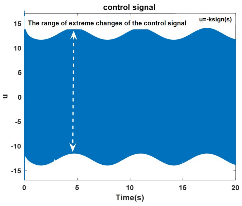	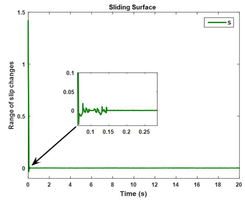
Variable structure	Control Signal	Sliding surface
$U_{SW} = -Kep\_sign(s)$	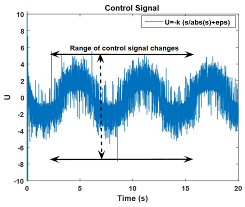	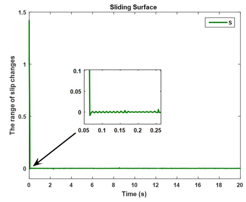
Variable structure	Control Signal	Sliding surface
$U_{SW} = -Ksat(s)$	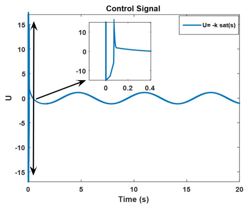	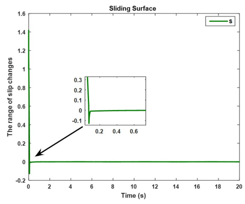
Variable structure	Control Signal	Sliding surface
$U_{SW} = -K\tanh(s)$	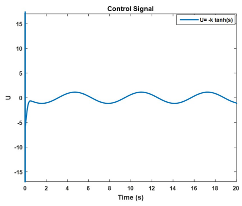	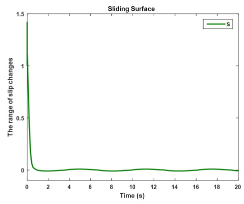
Variable structure	Control Signal	Sliding surface
$U_{SW} = -K\tanh(\frac{s}{\delta})$	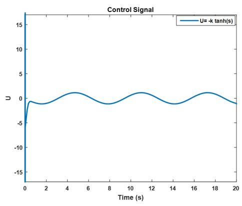	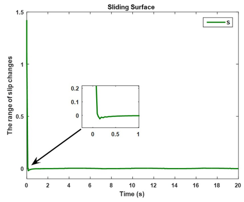
Variable structure	Control Signal	Sliding surface
$U_{ST} = -\lvert\alpha\rvert^{p} sign(s) + U_1$ $\dot{U}_1 = -\omega sign(s)$	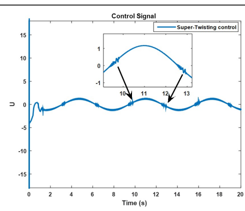	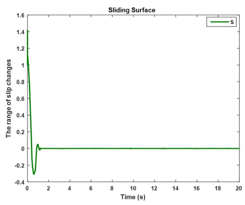
Variable structure	Control Signal	Sliding surface
$U_{SW} = -K\tanh(\rho s), k > 0$	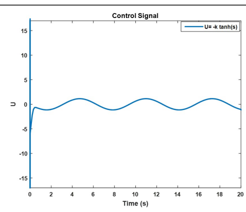	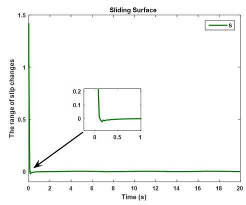

Table 4: Comparison of different methods in terms of the speed of reaching and absorbing the sliding surface

response specification	$-Ksign(s)$	$-Kep-sign(s)$	$-Ksat(s)$	$-K\tanh(s)$
Convergence time to sliding surface	$5s$	$10s$	$10s$	$> 20s$
Error when reaching the sliding surface	0.0003	$3.51E-5$	$3.96E-5$	0.0073

response specification	$-K\tanh(\frac{s}{\delta})$	$-K\tanh(\rho s)$	Super Twisting
Convergence time to sliding surface	$> 20s$	$> 20s$	$2s$
Error when reaching the sliding surface	0.00048	0.0261	$3.038E-6$

Table 5:

state variables and the reference signal. The figure below shows the performance of various functions and the sliding mode control method, how the system modes act in pursuit of the desired input signal.

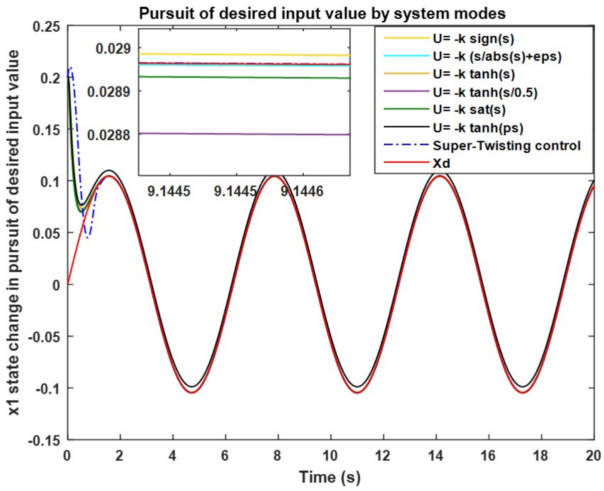

Figure 6: Reference tracking by x_1, using controlling structures of table 2

In Figure 6, the lowest amount of error and the best accuracy is related to the Super-Twisting control method, which completely and with negligible error follows the desired input signal by x1. To describe the performance of the above methodsmore precisely, in Table 5, a functional analysis of the control method is reviewed in terms of steady-state error, reaching time, the amount of overshoot of the control signal, the chattering range and the MSE error. Where the parameter N is sampled point numbers.

$$MSE = \frac{1}{N}\sum_{i=1}^{n}(X - X_d)^2 \tag{2.11}$$

According to Table 5, in terms of accuracy and covergence speed the Super-Twisting method shows a very good performance. Also, the overshoot values and changes in the control signal range are acceptable in this method, and it was able to control and eliminate the chattering phenomenon. Also, in the MSE section, a much better improvement can be made in the Super-Twisting method by adjusting the parameters, but a chattering phenomenon appears. In Figure 7 only the function $u = -ksign(s)$ cannot effectively track the desired input signal due to the excessive chattering phenomenon. The undesired chattering phenomenon is clearly shown in zoom-in window.

2.4 Controller design based on back stepping super twisting sliding mode control

Back stepping control technique is widely used to achieve the goals of industrial nonlinear system control including military equipment, robotics, medical engineering and technical services[6].

Theorem 2.2. Consider the nonlinear system 2.2 . The stable back stepping super twisting SMC controller is designed as:

$$u = \frac{1}{b}\left(-f + c_1\dot{e}_1 + \ddot{x}_d + c_2 s + ksign\left(s\right)\right) \tag{2.12}$$

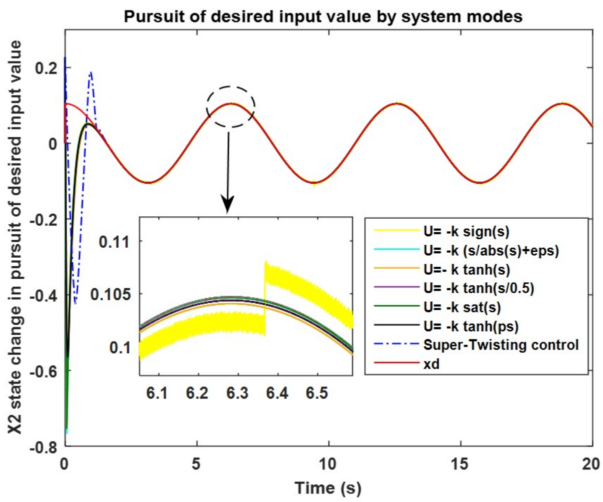

Figure 7: Reference tracking by x_2, using controlling structures of Table 2

$$u = \frac{\frac{4}{3}(M+m)L - mL\cos^2 x_1}{\cos x_1}\left(-\frac{(M+m)g\sin x_1 - mLx_2^2(\sin x_1\cos x_1)}{\frac{4}{3}(M+m)L - mL\cos^2 x_1} + c_1\dot{e}_1 + \ddot{x}_d + c_2 s + ksign(s)\right)$$

Proof . Consider the tracking error of state x_1 as follow:

$$e_1 = x_d - x_1 \quad , \quad \dot{e}_1 = \dot{x}_d - \dot{x}_1 = \dot{x}_d - x_2 \tag{2.13}$$

The positive definite Lyapunov function is defined as:

$$v_1 = \frac{1}{2}e_1^2 \tag{2.14}$$

and its related derivative is:

$$\dot{v}_1 = e_1\dot{e}_1 = e_1(\dot{x}_d - x_2). \tag{2.15}$$

To guarantee $\dot{V}_1 \leq 0, x_2$ is defined as follow:

$$x_2 = -s + c_1 e_1 + \dot{x}_d. \tag{2.16}$$

Considering above relation, sliding surface is proposed as follow:

$$s = c_1 e_1 + \dot{x}_d - x_2 = c_1 e_1 + \dot{e}_1, c_1 > 0. \tag{2.17}$$

Replacing 2.16 in 2.15 yields:

$$\dot{v}_1 = e_1(\dot{x}_d - (-s + c_1 e_1 + \dot{x}_d)) = e_1 s - c_1 e_1^2. \tag{2.18}$$

Consequently 2.19 results by deriving 2.17 :

$$\dot{s} = c_1\dot{e}_1 + \ddot{e}_1 = c_1\dot{e}_1 + \ddot{e}_1 = c_1\dot{e}_1 + \ddot{x}_d - \dot{x}_2, \tag{2.19}$$

where 2.19 is rewritten by 2.20:

$$\dot{s} = c_1\dot{e}_1 + \ddot{x}_d - f - bu \tag{2.20}$$

$$\dot{s} = c_1\dot{e}_1 + \ddot{x}_d - \frac{(M+m)g\sin x_1 - mLx_2^2(\sin x_1\cos x_1)}{\frac{4}{3}(M+m)L - mL\cos^2 x_1} - \frac{\cos x_1}{\frac{4}{3}(M+m)L - mL\cos^2 x_1}u.$$

In the second step Lyapunov function v2 is defined as:

$$v_2 = v_1 + \frac{1}{2}s^2. \tag{2.21}$$

Deriving 2.21, u is appeared and should be denoted such that it satisfies $\dot{V}_2 < 0$

$$\dot{v}_2 = \dot{v}_1 + s\dot{s} = e_1 s - c_1 e_1^2 + s\left(c_1 \dot{e}_1 + \ddot{x}_d - f - bu\right). \tag{2.22}$$

Accordingly, u will be calculated by relation 2.23:

$$u = \frac{1}{b}\left(-f + c_1 \dot{e}_1 + \ddot{x}_d + c_2 s + ksign\left(s\right)\right) \tag{2.23}$$

$$u = \frac{\frac{4}{3}(M+m)L - mL\cos^2 x_1}{\cos x_1}\left(-\frac{(M+m)g\sin x_1 - mLx_2^2(\sin x_1 \cos x_1)}{\frac{4}{3}(M+m)L - mL\cos^2 x_1} + c_1\dot{e}_1 + \ddot{x}_d + c_2 s + ksign\left(s\right)\right)$$
$$\Rightarrow \dot{v}_2 = -c_1 e_1^2 - c_2 s^2 + s - k\left|s\right| \le 0.$$

□

3 Simulation results

In this section, simulation is done to check the performance of the designed controller in terms of tracking modes, reducing chattering and reaching time.

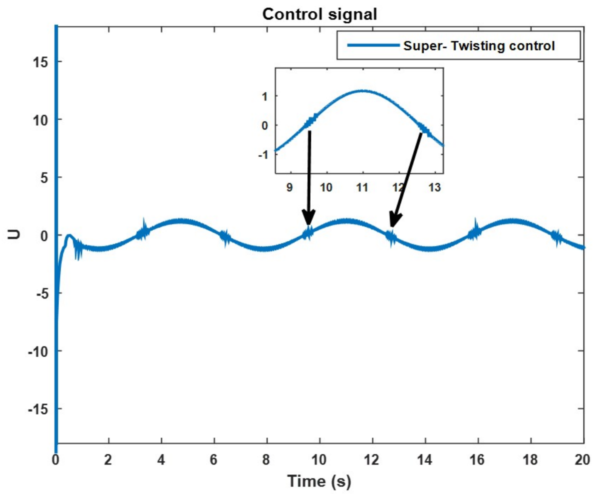

Figure 8: Control signal in backstepping Super Twisting SMC

Comparing Figure 8 with Table 3 it is clear that backstepping super twisting SMC contains less surge in specified points.

Additionally comparative results of Table 3 and Figure 9 shows better convergence of sliding surface to zero in proposed method. Considering Figure 10 it is clear that proposed method performs less convergence time.To better examine how the state variables move towards the input reference signal, in Figure 11, this tracking operation is drawn in 2D and the time to reach the desired value of the input reference signal is specified.

Finally Figure 12 indicates the tracking errors

Table 6 represents a brief comparison between feedback linearization, Super-Twisting SMCand back stepping-Super Twisting.

According to Table 6, in terms of the accuracy and states' convergence speed, the Backstepping Super twisting method shows very good performance and exact converges to the reference signal. In addition, it not only reduces the overshoot value but also can control and eliminate the chattering phenomenon. Considering the MSE section, we come to the conclusion that the backstepping - Super Twisting method has the lowest MSE value compared to the other methods, mentioned in Table 6.

As can be seen in Figure 13, the state variables in the back stepping Super Twisting method reach the sliding surface in less than 1s and remain on sliding surface. This indicates the efficiency of the control signal.

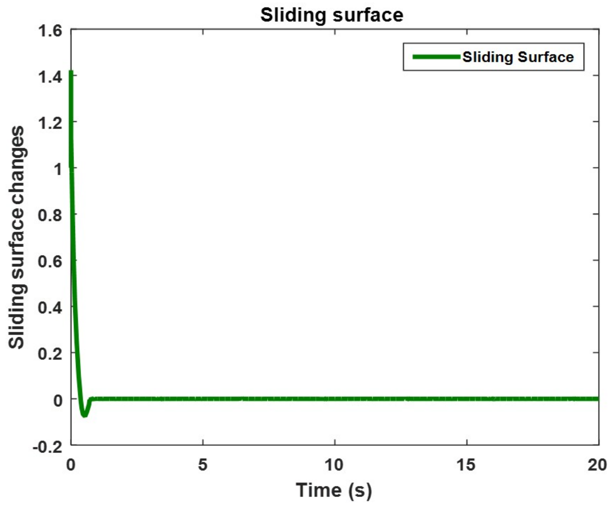

Figure 9: Sliding surface in Backstepping SuperTwisting method

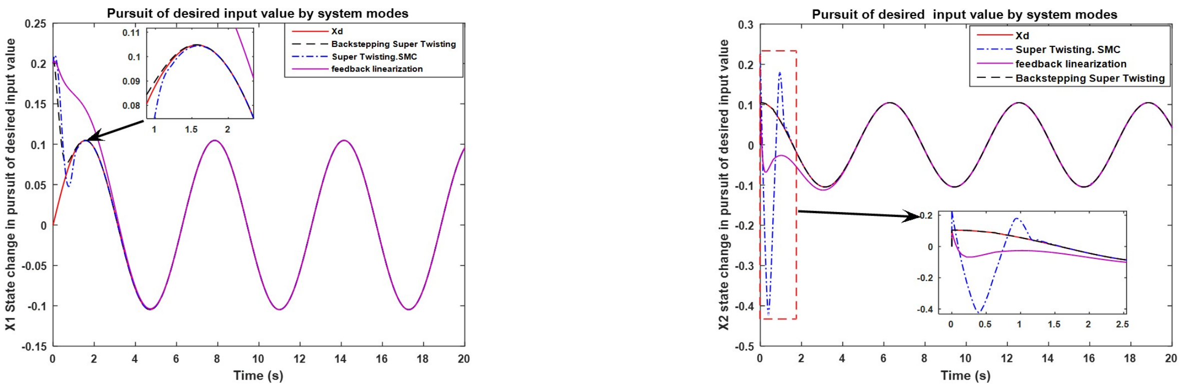

Figure 10: Comparative results of reference tracking

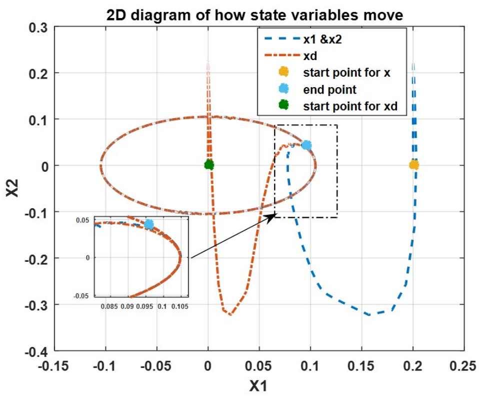

Figure 11: 2D diagram of reference tracking

In Table 7, Figure13 is analysed.

In Table 7, Super Twisting-SMC and Back stepping- Super twisting methods are compared in terms of convergence time to sliding surface with an error less than 0.0001. As can be seen in Table 7, in the Backstepping Super-Twisting method, the state variables reached the sliding surface very quickly and were not separated from the sliding surface until the end of the simulation time.

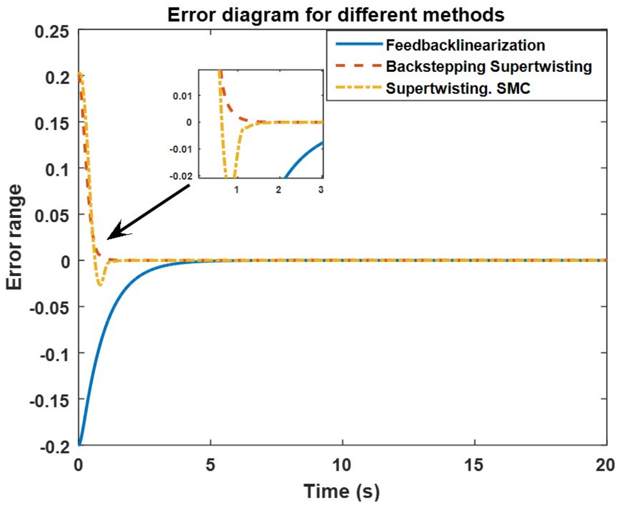

Figure 12: How to minimize the tracking error of the input reference signal in different ways

response specification	Steady state error	Time to reach the desired value(sec)	Over shoot(u)	The peak-to-peak amplitude of the u signal	MSE
Feedback linearization	0.0003	< 8	1.23	2.48	125.752
Super Twisting . SMC	0	< 2	1.7	2.35	0.0101
Backstepping - Super twisting	0	< 1.4	1.7	2.35	0.0042

Table 6: Performance analysis of control strategies

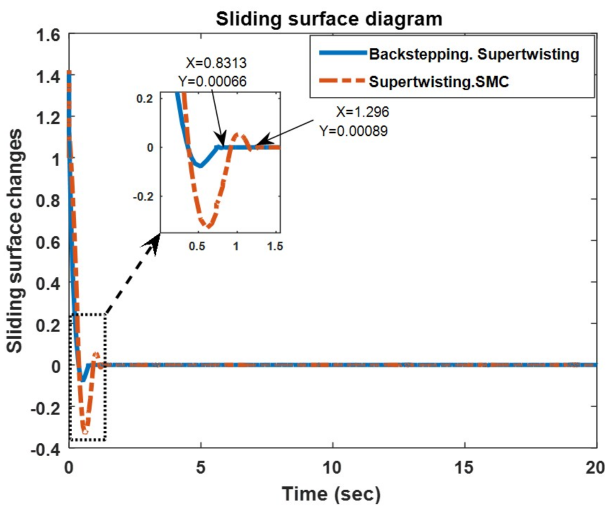

Figure 13: Sliding surface in Back stepping- Super Twisting method and Super Twisting-SMC method

4 Conclusion

In this article, a new super-twisting back-stepping sliding mode controller is proposed and to validate the performance of this controller, the outcome of some well-known nonlinear controlling techniques such as feedback linearization and super twisting SMC are compared in two aspects of controlling a specified class of nonlinear systems and removing the chattering phenomenon. Also, the results are compared not only in clear schematicfigures but also analyzed in quantitative detail. In addition, the stability analysis of the closed-loop system is presented according to the Lyapunov theorem. The results clearly show the efficiency of the proposed method.In future works, to improve the performance of the proposed method in the sense of convergence speed section, It is recommended to combine the super-twisting

Table 7: Comparison of different methods in terms of the speed of reaching and absorbing the sliding surface

response specification	Back stepping Super Twisting	Supper Twisting - SMC
Convergence time to sliding surface	1S	2S
Error when reaching the sliding surface	5.94E-5	2.2E-5

back-stepping with advanced sliding mode methods such as terminal SMC or fast terminal SMC to improve the convergence time. Also, the sensitivity of system to the noise and disturbance can be discussed and calculated.

References

[1] R. Abedzadeh Maafi, S. Etemadi Haghighi, and M.J. Mahmoodabadi, *Pareto optimal design of a fuzzy adaptive hierarchical sliding-mode controller for an XZ inverted pendulum system*, IETE J. Res. **69** (2021), no. 5, 3052–3069.

[2] R. Afifa, S. Ali, M. Pervaiz, and J. Iqbal, *Adaptive backstepping integral sliding mode control of a mimo separately excited DC motor*, Robotics **12** (2023), no. 4, 1–16.

[3] W. Alam, A. Mehmood, Kh. Ali, U. Javaid, S. Alharbi, and J. Iqbal, *Nonlinear control of a flexible joint robotic manipulator with experimental validation*, J. Mech. Engin. **64** (2018), no. 1, 47–55.

[4] Kh.A. Alattas, O. Mofid, A.K. Alanazi, H.M. Abo-Dief, A. Bartoszewicz, M. Bakouri, and S. Mobayen, *Barrier function adaptive nonsingular terminal sliding mode control approach for quad-rotor unmanned aerial vehicles*, Sensors **72** (2022), no. 3, 1–20.

[5] S. Ali, A. Prado, and M. Pervaiz, *Hybrid backstepping-super twisting algorithm for robust speed control of a three-phase induction motor*, Electronics **12** (2023), no. 3.

[6] K. Ali, L. Khan, Q. Khan, Sh. Ullah, S. Ahmad, S. Mumtaz, F. Karam, and Naghmash, *Robust integral backstepping based nonlinear MPPT control for a PV system*, Energies **12** (2019), no. 16.

[7] D.J. Almakhles, *Robust backstepping sliding mode control for a quadrotor trajectory tracking application*, IEEE Accsess **8** (2020), 5515–5525.

[8] M. Andalib Sahnehsaraei and M.J. Mahmoodabadi, *Approximate feedback linearization based optimal robust control for an inverted pendulum system with time-varying uncertainties*, Int. J. Dyn. Control **9** (2021), 160–172.

[9] J. Ansari, M. Homayounzade, and A. Abbasi, *Load frequency control in power systems by a robust backstepping sliding mode controller design*, Energy Rep. **10** (2023), 1287–1298.

[10] G.R. Ansarifar and H.R. Akhavan, *Sliding mode control design for a PWR nuclear reactor using sliding mode observer during load following operation*, Ann. Nuclear Energy **75** (2015), 611–619.

[11] S. Coskun, *Non-linear control of inverted pendulum*, J. Faculty Engin. Architect. **35** (2020), 27–38.

[12] Y. Dong, G. Zhang, G. He, and W. Si, *A novel control strategy for uninterruptible power supply based on backstepping and fuzzy neural network*, IEEE Access **11** (2023), 5306–5313.

[13] H. Eddine Glida, L. Abdou, A. Chelihi, Ch. Sentouh, and S. Hasseni, *Optimal model-free backstepping control for a quadrotor helicopter*, Nonlinear Dyn. **100** (2020), 3449–3468.

[14] S. Hassan, B. Abdelmajid, Z. Mourad, S. Aicha, and B. Abdennaceur, *PSO-backstepping controller of a grid connected DFIG based wind turbine*, Int. J. Electric. Comput. Engin. **10** (2020), no. 1, 856–867.

[15] J. Hu, H. Zhang, H. Liu, and X. Yu, *A survey on sliding mode control for networked control systems*, Int. J. Syst. Sci. **52** (2021), no. 6, 1129–1147.

[16] J. Huang, T. Zhang, Y. Fan, and J.Q. Sun, *Control of rotary inverted pendulum using model-free backstepping technique*, IEEE Access **7** (2019), 96965–96973.

[17] S. Irfan, A. Mehmood, M. Tayyab Razzaq, and J. Iqbal, *Advanced sliding mode control techniques for inverted pendulum: Modelling and simulation*, Engin. Sci. Technol. Int. J. **72** (2018), no. 4, 753–759.

[18] O. Jedda, J. Ghabi, and A. Douik, *Sliding mode control of an inverted pendulum*, Chapter 6, Research Gate, 2017.

[19] A.A. Kabanov, *Feedback linearization of nonlinear singularly perturbed Systems with state-dependent coefficients*, Int. J. Control Autom. Syst. **18** (2020), 1743–1750.

[20] K. Kayisli and R.Z. Caglayan, *Twisting sliding mode control based maximum power point tracking*, Balkan J. Electric. Comput. Engin. **10** (2022), no. 4, 356–362.

[21] Y. Lan and F. Minrui, *Design of state-feedback controller by pole placement for a coupled set of inverted pendulums*, Tenth Int. Conf. Electronic Measure. Instruments, IEEE, 2011, pp. 68–72.

[22] Sh. Li, M. Zhou, and X. Yu, *Design and implementation of terminal sliding mode control method for PMSM speed regulation system*, IEEE Trans. Ind. Inf. **9** (2011), no. 4, 1879–1891.

[23] Y. Liang, D. Zhang, G. Li, and T. Wu, *Adaptive chattering-free PID sliding mode control for tracking problem of uncertain dynamical systems*, Electronics **11** (2022), no. 21, 1–18.

[24] X. Liu, X. Xu, Z. Zhu, and Y. Jiang, *Dual-arm coordinated control strategy based on modified sliding mode impedance controller*, Sensors **21** (2021), no. 14, 2–22.

[25] W. Liu, H. Ye, and X. Yang, *Super-twisting sliding mode control for the trajectory tracking of underactuated USVs with disturbances*, J. Marine Sci. Engin. **11** (2023), no. 3, 1–15.

[26] Zh. Ma and Q. Yu, *Control strategy for boost converter based on adaptive integral terminal sliding-mode control*, J. Phys.: Conf. Ser. **2378** (2022), 1–7.

[27] M.J. Mahmoodabadi and M. Andalib Sahnehsaraei, *Parametric uncertainty handling of underactuated nonlinear systems using an online optimal input-output feedback linearization controller*, Syst. Sci. Control Engin. **9** (2021), no. 1, 209–218.

[28] M.S. Mahmoud, Radhwan A.A. Saleh, and A. Ma'arif, *Stabilizing of inverted pendulum system using Robust sliding mode control*, Int. J. Robot. Control Syst. **2** (2022), no. 2, 230–239.

[29] B. Majout, B. Bossoufi, M. Bouderbala, M. Masud, J.F. Al-Amri, M. Taoussi, M. El Mahfoud, S. Motahhir, and M. Karim, *Improvement of PMSG-based wind energy conversion system using developed sliding mode control*, Energies **15** (2022), no. 5, 1–17.

[30] S. Mobayen, *Adaptive global sliding mode control of underactuated systems using a super-twisting scheme: An experimental study*, J. Vib. Control **25** (2019), no. 16, 1-19.

[31] S. Mobayen, A. Fekih, S. Vaidyanathan, and A. Sambas, *Chameleon chaotic systems with quadratic nonlinearities: An adaptive finite-time sliding mode control approach and circuit simulation*, IEEE Access **9** (2021), 64558–64573.

[32] S. Mobayen, F.Tchier, and L. Ragoub, *Design of an adaptive tracker for n-link rigid robotic manipulators based on super-twisting global nonlinear sliding mode control*, Int. J. Syst. Sci. **48** (2017), no. 9, 1990–2002.

[33] A. Nagarajan and A.A. Victoire, *Optimization reinforced PID-sliding mode controller for rotary inverted pendulum*, IEEE Access **11** (2023), 24420–24430.

[34] B.B. Naik and A.J. Mehta, *Sliding mode controller with modified sliding function fo rDC-DC Buck converter*, ISA Trans. **20** (2017), 279–287.

[35] P. Nam Dao and Y. Chen Liu, *Adaptive reinforcement learning strategy with sliding mode control for unknown and disturbed wheeled inverted pendulum*, Int. J. Control Automat. Syst. **19** (2021), 1139–1150.

[36] N.P. Nguyen, H. Oh, Y. Kim, J. Moon, J. Yang, and W. Chen, *Fuzzy-based super-twisting sliding mode stabilization control for under-actuated rotary inverted pendulum systems*, IEEE Access **8** (2020), 185079–185092.

[37] A. Norouzi, M. Masoumi, A. Barari, and S. F. Sani, *Lateral control of an autonomous vehicle using integrated backstepping and sliding mode controller*, Proc. Inst. Mech. Engin. Part K: J. Multi-body Dyn. **233** (2019), no. 1, 141–151.

[38] A.K. Patra, S.S. Biswal, and P. Kumar Rout, *Backstepping linear quadratic Gaussian controller design for balancing an inverted pendulum*, IETE J. Res. **68** (2019), no. 1, 150–164.

[39] B. Qiu, G. Wang, Y. Fan, D. Mu, and X. Sun, *Adaptive sliding mode trajectory tracking control for unmanned*

surface vehicle with modeling uncertainties and input saturation, Appl. Sci. **9** (2019), no. 6, 1–18.

[40] Z. Qiu and S. Zhang, *Fuzzy fast terminal sliding mode vibration control of a two-connected flexible plate using laser sensors*, J. Sound Vibr. **380** (2016), 51-77.

[41] R. Saravanakumar and D. Jena, *Validation of an integral sliding mode control for optimal control of a three blade variable speed variable pitch wind turbine*, Electric. Power Energy Syst. **69** (2015), 421–429.

[42] Ch. Song, Sh. Fei, J. Cao, and Ch. Huang, *Robust synchronization of fractional-order uncertain chaotic systems based on output feedback sliding mode control*, Mathematics **7** (2019), no. 7, 2–10.

[43] L. Yu, J. Huang, W. Luo, Sh. Chang, H. Sun, and H. Tian, *Sliding-mode control for PMLSM position control*, Actuators **12** (2023), no. 1, 1–23.

[44] F.M. Zaihidee, S. Mekhilef, and M. Mubin, *Robust speed control of PMSM using sliding mode control (SMC)-A review*, Energies **12** (2019), no. 9, 1–27.

[45] A.R. Zare and M. Ahmadizadeh, *Modified sliding mode design of passive viscous fluid control systems for nonlinear structures*, Engin. Struct. **162** (2018), 245–256.

[46] S. Zeghlache, M.Z. Ghellab, A. Djerioui, B. Bouderah, and M.F. Benkhoris, *Adaptive fuzzy fast terminal sliding mode control for inverted pendulum-cart system with actuator faults*, Math. Comput. Simul. **210** (2023), 207–234.

[47] M. Zhang, J. Huang, and Y. Cao, *Adaptive super-twisting control for mobile wheeled inverted pendulum systems*, Appl. Sci. **9** (2019), no. 12.

[48] J. Zhang, N. Zhang, G. Shen, and Y. Xia, *Analysis and design of chattering-free discrete-time sliding mode control*, Int. J. Robust Nonlinear Control **29** (2019), no. 18, 6572–6581.

[49] M. Zhihong and X. Huo Yu, *Terminal sliding mode control of MIMO linear systems*, IEEE Trans. Circ. Syst. **44** (1997), no. 11, 1065–1070.